



HAL
open science

Urbanization and hydrological conditions drive the spatial and temporal variability of microplastic pollution in the Garonne River

Aline Reis de Carvalho, Flavien Garcia, Louna Riem-Galliano, Loïc Tudesque, Magali Albignac, Alexandra ter Halle, Julien Cucherousset

► To cite this version:

Aline Reis de Carvalho, Flavien Garcia, Louna Riem-Galliano, Loïc Tudesque, Magali Albignac, et al.. Urbanization and hydrological conditions drive the spatial and temporal variability of microplastic pollution in the Garonne River. *Science of the Total Environment*, 2021, 769, pp.144479. 10.1016/j.scitotenv.2020.144479 . hal-03211025

HAL Id: hal-03211025

<https://hal.science/hal-03211025v1>

Submitted on 13 Feb 2023

HAL is a multi-disciplinary open access archive for the deposit and dissemination of scientific research documents, whether they are published or not. The documents may come from teaching and research institutions in France or abroad, or from public or private research centers.

L'archive ouverte pluridisciplinaire **HAL**, est destinée au dépôt et à la diffusion de documents scientifiques de niveau recherche, publiés ou non, émanant des établissements d'enseignement et de recherche français ou étrangers, des laboratoires publics ou privés.



Distributed under a Creative Commons Attribution - NonCommercial 4.0 International License

1 **Urbanization and hydrological conditions drive the spatial and**
2 **temporal variability of microplastic pollution in the Garonne**
3 **River**

4
5 Aline Reis de Carvalho^{1,2*}, Flavien Garcia^{1,2}, Louna Riem-Galliano², Loïc Tudesque²,
6 Magali Albignac¹, Alexandra ter Halle¹ and Julien Cucherousset²

7
8 ¹ UMR 5623 IMRCP (Laboratoire des Interactions Moléculaires et Réactivité Chimique
9 et Photochimique), CNRS, Université Toulouse III Paul Sabatier, 118 route de
10 Narbonne, 31062 Toulouse, France

11
12 ² UMR 5174 EDB (Laboratoire Évolution and Diversité Biologique), CNRS, Université
13 Toulouse III Paul Sabatier, 118 route de Narbonne, 31062 Toulouse, France

14
15 * Corresponding author: carvalho@chimie.ups-tlse.fr

16

17 **Abstract**

18 Microplastic (MP) pollution represents a novel environmental pressure acting on
19 freshwater ecosystems. Improving our understanding of the dynamics of MP pollution
20 in freshwater ecosystems is therefore a prerequisite for managing and limiting this
21 pollution. In this study, we quantified the spatial and temporal variability of MP (size
22 range 700 μm – 5 mm) pollution in surface water in 14 sites located across the
23 Garonne river catchment (Southwestern France, 6 in the main river and 8 tributaries).
24 MP concentration averaged 0.15 particles.m⁻³ (\pm 0.46 SD) and strongly varied both in
25 space and in time. We found that the spatial variation in MP concentration was driven
26 by urbanization and that the temporal variation in MP concentration and MP size was
27 driven by hydrological conditions, with higher concentrations and smaller particles sizes
28 in warm seasons with low discharge. Polyethylene (44.5%), polystyrene (30.1%) and
29 polypropylene (18.2%) were the main polymers and their proportion did not vary
30 significantly across sampled sites. Particle color was associated with polymer type, with
31 a high proportion of white particles in polystyrene. We also found a significant and
32 negative relationship between MP size and the distance to the source in sites located
33 in the main stream. MP pollution across watersheds, from headwater tributaries to
34 lowland rivers, is dynamic, and further studies are needed to improve our knowledge of
35 spatial and temporal patterns of MP pollution in freshwater ecosystems.

36

37 **Keywords:** freshwater, plastic pollution, polymer, surface water, microplastic color,
38 microplastic size.

39

40 **1. Introduction**

41 Freshwater ecosystems provide countless services to humans, but they are facing
42 multiple disturbances induced by global changes (Vörösmarty et al., 2010). Habitat
43 fragmentation (Morita et al., 2009), water pollution (Couceiro et al., 2007), climate
44 changes (Magnuson et al., 1997) and biological invasions (Gallardo et al., 2016) are
45 among the multiple factors threatening freshwater ecosystems and their rich
46 biodiversity. Microplastic (MP) pollution has recently emerged as a novel source of
47 concern with potential effects on freshwater biodiversity and ecosystems that remain to
48 be quantified (Eerkes-Medrano et al., 2015; Eerkes-Medrano and Thompson, 2018).
49 Rivers are at the heart of the dynamic of plastic pollution (Rochman, 2018), notably
50 because they convey 70-80% of the plastics observed in marine ecosystems (Horton et
51 al., 2017). In aquatic environment, plastics undergo a degradation process through
52 mechanical abrasion, photochemical alteration and other weathering processes
53 (Andrady, 2011; Gewert et al., 2015; ter Halle et al., 2017) which leads to the
54 production of MP, i.e. plastic fragments smaller than 5 mm (Arthur et al., 2009;
55 Thompson et al., 2009). In addition, primary MPs (i.e. those not originated by
56 fragmentation of larger debris) often found as cosmetics additives and drug vectors
57 (Cole et al., 2011) can directly enter freshwater ecosystems.

58 MP pollution is an ubiquitous phenomenon (Lusher et al., 2015; Rochman,
59 2018; Woodall et al., 2014) and the presence and accumulation of MP in ecosystems
60 represent an important toxicological risk for organisms through direct and indirect
61 ingestion (Prata et al., 2020; Smith et al., 2018). The study of MP properties, such as
62 composition, density, size and color, can not only contribute to elucidate their origins,
63 but also provides insights into the drivers of their consumption by aquatic organisms
64 (Collard et al., 2019; Wang et al., 2019). MP can be ingested across many freshwater
65 consumers taxa, from invertebrates (Windsor et al., 2019) to fish (McNeish et al., 2018;
66 Roch et al., 2019; Sloopmaekers et al., 2019) and the consequences of MP

67 consumption on individual organisms are highly variable (Foley et al., 2018). Although
68 there has been a recent increase in the number of studies investigating MP pollution in
69 freshwater ecosystems, improving our understanding of the dynamics of this pollution
70 in these ecosystems is essential (Eerkes-Medrano and Thompson, 2018; Horton et al.,
71 2017).

72 In rivers, MP pollution varies spatially and is strongly affected by land use
73 (Skalska et al., 2020). Urbanization is a key driver of MP pollution in freshwater
74 ecosystems (Baldwin et al., 2016; Cable et al., 2017; Grbić et al., 2020), and, in highly
75 urbanized areas, MP contamination levels are comparable to those observed in marine
76 environments (Horton et al., 2017). However, our knowledge of the effects of different
77 land use practices on the characteristics of MP pollution remains limited, and MP
78 composition has already been identify as an approach to identification of microplastic
79 sources (Chen et al., 2020). MP pollution can also vary temporally through changes in
80 hydrological and meteorological conditions. Indeed, flood and rainfall can regulate the
81 mobilization of particles previously settled in sediments or on land (Zhang et al., 2017).
82 For instance, MP pollution can be affected by weather conditions and increase after
83 precipitation events (Eo et al., 2019) and several studies have demonstrated a positive
84 correlation between rainfall rates and MP pollution (Cheung et al., 2019; Dris et al.,
85 2015; Wong et al., 2020; Yonkos et al., 2014). The effects of seasonal variability are
86 more ambiguous, with studies showing either the presence (Han et al., 2020; Wu et al.,
87 2019) or the absence (Mani and Burkhardt-Holm, 2019; Rodrigues et al., 2018) of
88 seasonal patterns. Despite its importance for the development of efficient management
89 strategies on MP pollution in freshwater ecosystems, integrative quantification and
90 characterization of MP pollution and comprehensive analyses of its spatial and
91 temporal drivers are lacking (Lebreton et al., 2017; Li et al., 2020).

92 The present study aims to fill this gap of knowledge by quantifying the
93 environmental determinants of the spatial and temporal variability of MP pollution
94 (particles with a size range from 700 μm to 5mm) in surface water of the Garonne river

95 (South-western France). We first quantified the changes in MP concentration across
96 studied sites and sampling events. We tested the hypothesis that MP concentration
97 was variable spatially and temporally and associated to changes in environmental
98 conditions. The variability in environmental conditions between sampling sites and
99 events was quantified using a multivariate approach. Second, we investigated the
100 spatial and temporal changes in MP composition. We tested the hypothesis that MP
101 composition was different between sampling sites but not between sampling events
102 and correlated with changes in environmental conditions. Third, we explored changes
103 in MP size and hypothesized that MP size varied in time and space, and that this
104 variation was related with changes in environmental conditions. We also tested if there
105 was an overall size difference between MP polymers. Finally, we quantified changes in
106 MP size along the upstream-downstream gradient in the main river.

107

108 **2. Materials and methods**

109 **2.1 Study area and sampling design**

110 This study was performed in the Garonne river catchment, located in southwestern
111 France. The Garonne river is the third largest French river with a mean annual
112 discharge of $630 \text{ m}^3 \cdot \text{s}^{-1}$. It drains about 53.536 km^2 and the main channel flows
113 northwards over 525 km from its source in central Pyrenees in Spain to the Atlantic
114 Ocean nearby Bordeaux, France (**Fig. 1**). It flows through the large city of Toulouse.
115 Discharge is strongly dependent on snowmelt and is also influenced by precipitations,
116 typically resulting in a flood peak in May-June and a period of low flow from summer to
117 early autumn (Lambs et al., 2009; Maire et al., 2013).

118 Fourteen sampling sites distributed across the Garonne basin were selected to
119 cover the entire spatial heterogeneity in river characteristics and a large gradient of
120 land use (**Fig. 1 and Supplementary Table S1**). Six sites were located on the main
121 stream of the Garonne river (from upstream to downstream: LBA, LBI, MUG, GSG,

122 CAS and AGE; **Fig. 1**). Eight sites were located in the downstream part (before flowing
123 into the main stream) of some of the main tributaries of the Garonne river (from
124 upstream to downstream: SLN in the river Neste, RSG in the river Salat, MUL in the
125 river Louge, GRP in the river Ariège, LAU in the river Hers, TOU in the river Touch,
126 GRN in the river Save and LAY in the river Gers).

127 All sites were sampled at four occasions: February 13 to 15, April 23 to 26, July 01
128 to 04 and October 07 to 09, 2019, to represent seasonal variability in discharge
129 (**Supplementary Fig. S1 and Supplementary Table S2**). On average, 3 to 5 sites
130 were sampled per day, with a duration of approximately 2 hours per site.

131 MP were sampled by filtering surface water using a Manta trawl (32 cm x 82
132 cm) equipped with a polyamide net (mesh size of 500 μm) and a removable cod-end
133 with the same mesh size (Faure et al., 2012; Galgani et al., 2013; Hidalgo-Ruz et al.,
134 2012). Each sampling event consisted in attaching the Manta trawl to the bridge
135 guardrail over the river and by immersing it in the fast flowing and deepest parts of
136 each site for approximately 10 minutes (sampling duration was recorded to the nearest
137 second for each sampling). Sampling of each site was replicated three times at each
138 sampling event with all replicates being performed successively, leading to a total of
139 168 samples (4 events x 14 sites x 3 replicates). The net entrance was equipped with a
140 mechanical flowmeter (Hydro-Bios, Germany) placed at its center to estimate the
141 volume of filtered water during the sampling duration. The average volume of filtered
142 water was 99.6 m^3 (\pm 53.7 SD) and ranged from to 4.25 m^3 to 259.1 m^3 depending on
143 the sampling site and the sampling event (**Supplementary Table S3**). After each
144 sampling, the cod-end content was sieved into a 500 μm mesh using river water and
145 transferred to sealable plastic bags (e.g. Cheung et al., 2019; Wong et al., 2020). Due
146 to the particle size range considered in the present study, contamination from these
147 bags was very unlikely. Samples were stored in a cooler in the field and stocked at 4°C
148 in the laboratory before subsequent analyses.

149

150

151 **2.2 Sample processing**

152 In the laboratory, the sample processing was composed of five steps, consisting of 1)
153 sieving, 2) chemical digestion, 3) washing/filtration, 4) wet peroxidation and 5)
154 washing/filtration, representing an adaptation of existing methods (Dehaut et al., 2016;
155 Hurley et al., 2018; Rodrigues et al., 2018). Samples were first transferred into a sieve
156 (mesh size of 500 μm) to remove large debris (> 1 cm) such as tree leaves and
157 branches that were abundantly rinsed with water. The remaining content was
158 transferred into 250 mL glass bottles. Screw caps with aperture (Schott Duran®, DWK
159 Life Sciences, Germany) equipped with polyamide fabric of 500 μm mesh (Nitex®,
160 SEFAR, Switzerland) were used to close the bottles. Chemical digestion was then
161 performed by incubating each sample with enough potassium hydroxide (KOH)
162 (pellets, Sigma-Aldrich, USA) solution 10% (w/w) to cover the sample in a water bath
163 (60°C) for 8 hours under intermittent agitation. The sample was filtered through the
164 Nitex® and rinsed with distilled water. A wet peroxidation was carried out by adding
165 enough hydrogen peroxide (H_2O_2) solution (Merck KGaA, Germany) 30% (w/w) to
166 cover the sample and incubating overnight at room temperature (Karlsson et al., 2017).
167 Samples were then finally filtered through the Nitex® and washed with distilled water.
168 The residue content at the Nitex® was stored in petri-dishes at room temperature until
169 further analyses.

170

171 **2.3 Identification and characterization of microplastic particles**

172 Particles identification was performed using stereomicroscope (Leica MZ 75 and Nikon
173 SMZ 800). Two consecutive inspections of each sample were performed independently
174 by two different operators. The first inspection took an average of 12.6 min (± 11.0 SD)

175 per sample and the second inspection lasted 5.5 min on average (± 3.8 SD). In total,
176 87% of all particles were detected during the first inspection. All particles ranging from
177 700 μm (diagonal of the 500 μm mesh net) to 5 mm identified as potentially plastic
178 particles were separated using metallic tweezers and stored in small petri dishes. Each
179 particle was subsequently photographed using a stereomicroscope (Leica MZ16)
180 equipped with a digital camera (DP20, Olympus, Japan) and classified into predefined
181 categories of colors, as black, white, blue, green, grey, red and yellow (Mani and
182 Burkhardt-Holm, 2019) (**Fig. 2**). The length of each particle were subsequently
183 measured on the pictures using the ImageJ software (Rasband, 1997), as the length of
184 its longest dimension (**Supplementary Fig. S2**).

185 The chemical characterization of each particle was performed by attenuated total
186 reflectance Fourier transformed infrared spectroscopy (ATR-FTIR, Thermo Nicolet
187 6700, Thermo Fisher Scientific) (Käppler et al., 2016) equipped with a diamond crystal.
188 The ATR crystal was cleaned with ethanol with a background scan prior to analysis of a
189 set of 24 particles. The IR spectra were obtained with a resolution of 4 cm^{-1} over the
190 wavenumber range from 400 to 4000 cm^{-1} applying 8 scans. Each spectrum was
191 compared with the reference spectra of synthetic polymers from commercially available
192 libraries using OMNIC software (Thermo Fisher Scientific). The similarity threshold of
193 70% was settled for the chemical composition to be assigned to the particle
194 (Huppertsberg and Knepper, 2020), otherwise it was considered as non-identified. The
195 identified particle was then classified as the polymer type (or polymer artificial additive),
196 based on the Polymer Properties Database (Polymer Database, 2020) when available,
197 or as non-plastic (**Supplementary Fig. S3**). The final categories of MP composition
198 were: polyethylene (PE), polypropylene (PP), polystyrene (PS), polyester (including
199 polyethylene terephthalate, PET), polyacrylate, polyvinylester, polyamide,
200 polyurethane, polydiene, polysiloxane, polyethersulfone, tire and bitumen MP particles
201 (TBMP) (Järskog, 2020; Leads and Weinstein, 2019) and artificial additives

202 (considered here as polyolefin-based or alkyd resins, as waxes, oils and coatings
203 lubricants (Hofland, 2012; Song et al., 2014; Su et al., 2020). The last two categories
204 were considered as microplastics (Hartmann et al., 2019), with the latter showing
205 similarities with paint particles (Verschoor et al., 2016). The ATR-FTIR spectra of
206 typical samples and the comparison with a database of spectra are displayed in
207 **Supplementary Fig. S4**. If the occurrence of a category was less than 5% of the total
208 number of plastics, it was then considered as “other” for further analyses.

209

210 **2.4 Quality assurance and quality control**

211 The potential effects of the treatment to digest organic matter on particles were
212 measured using raw microplastic pellets. Samples composed of three to five pellets
213 (size ranging from 1 to 5 mm) of the same polymer were analyzed in triplicates and a
214 total of twelve different polymers were tested (**Supplementary Table S4**). Mass
215 variation and chemical modification can be caused by chemical digestion and high
216 temperatures, resulting in misdetection or incorrect identification of particles. The
217 weight and ATR-FTIR spectra of each particle were obtained before and after the
218 treatment to digest organic matter. Results revealed that this treatment induced no
219 mass variation and no alterations of infrared spectra (**Supplementary Fig. S5**), leading
220 to unmodified match with reference library. Therefore, this protocol was considered as
221 robust for the present study.

222 To avoid any cross-site contamination, the sampling equipment was rinsed in
223 the river prior to the sampling of each site. In the laboratory, all material was previously
224 rinsed with distilled water and ethanol. Metal and glassware were used whenever
225 possible. All the procedure was performed under a hood and samples recipients
226 remained covered with original caps or aluminum foil. A cotton lab-coat and nitrile

227 gloves were always worn, and work surfaces were cleaned with ethanol. Fibers
228 particles were not included as MP particles considered in this study.

229

230

231 **2.5 Environmental conditions**

232 Environmental conditions in each sampling site and at each event were summarized
233 using multivariate analyses based on a series of spatial and temporal descriptors.
234 Environmental parameters related to water characteristics, as temperature and turbidity
235 (NTU – Nephelometric Turbidity Unit), were measured with a DO probe (ProDSS
236 Multiparameter Water Quality Meter, YSI, USA) at each sampling event and for each
237 site (**Supplementary Table S2**). Daily discharge of each site (except SLN that had no
238 gauge) were obtained from the Agence de l'Eau Adour-Garonne (HydroEauFrance,
239 2020) (**Supplementary Table S2**). Daily air temperature and precipitations were
240 obtained from Meteo France (MeteoFrance, 2020) (**Supplementary Table S5**). River
241 width was measured at each site using aerial pictures (Géoportail, 2020). A
242 Geographic Information System (ArcGIS v.10.6, ESRI, Redlands, CA, USA) was then
243 used to calculate, for each site, the distance to the Garonne river source, drainage
244 area, land cover (urban and agricultural) and human population. The distance to the
245 Garonne river source (km) was calculated between each sampling site and the source
246 of the Garonne river following the main river bed and the drainage area (km²)
247 represented the area of land drained in each site. Urban and agricultural land cover (%)
248 was calculated at a predetermined buffer scale of 5 km long with 1 km large upstream
249 of the each sampling site using the Corine Land Cover database (European
250 Environment Agency, 2018). Human population (numbers of inhabitants) was
251 calculated using the same buffer and sourced from the INSEE (INSEE, 2018) which
252 described the population in each municipality. Because municipality did not exactly

253 overlap with our buffer, we calculated the percentage of municipalities' area included in
254 the buffer to assess the numbers of inhabitants.

255

256

257

258 **2.6 Statistical analyses**

259 We first conducted two Principal Component Analyses (PCA) to summarize the spatial
260 and temporal variability in environmental conditions and avoid collinearity among
261 variables used to assess the environmental determinants of MP pollution. Regarding
262 environmental variability across sampling sites, 6 variables (namely river width,
263 drainage area, mean yearly discharge, human population, urban land cover and
264 agricultural land cover) were used. The first two axes of the PCA (eigenvalues of 3.06
265 and 2.31, respectively) represented 89.39% of the total inertia and were selected for
266 subsequent analyses (**Fig. 3a**). The first axis (PC1) was defined as river size as it was
267 strongly associated ($r > 0.60$) with river width, drainage area and mean yearly
268 discharge. This axis discriminated large sites located downstream in the Garonne river
269 with high discharge (e.g. AGE, CAS, GSG) from smaller sites, located upstream in the
270 Garonne river and its tributaries displaying lower discharge (e.g. LBA, GRN, LAY). The
271 second axis (PC2) was defined as the level of urbanization as it was strongly
272 associated ($r > 0.60$) with human population density, urban land cover and agricultural
273 land cover. This axis discriminated sites located in an agricultural landscape with low
274 human population density (e.g. LBI, SLN, GRP) from sites with high population density
275 located in highly urbanized area (e.g. LAU, TOU, GSG) (**Fig. 3b**).

276 Regarding environmental variability across sampling events, we used 7
277 variables in the PCA representing the temporal changes in environmental conditions:
278 water temperature, air temperature (day before sampling), precipitations the day before

279 sampling and cumulated across three days before sampling, relative turbidity
280 (calculated as the relative values across the 4 sampling events within each site),
281 relative discharge (calculated as the relative values across the 4 sampling events
282 within each site), and discharge fluctuation (relative change in discharge observed
283 within 3 days before sampling). The first two axes of the PCA (eigenvalues of 3.06 and
284 2.28, respectively) represented 76.33% of the total inertia and were selected for
285 subsequent analyses (**Fig. 4a**). The first axis (PC1) represented seasonal hydrological
286 conditions as it was strongly associated ($r > 0.60$) with relative discharge, relative
287 turbidity and air and water temperatures. This axis discriminated sampling events
288 performed in low discharge and turbidity conditions and with high air and water
289 temperatures (e.g. July) from events performed when discharge and turbidity were
290 high, and air and water temperatures were low (e.g. February). The second axis (PC2)
291 was strongly associated ($r > 0.60$) with precipitation that occurred 24 hours and 72
292 hours before sampling and changes in discharge, and was therefore defined as
293 weather changes. This axis discriminated sampling events that occurred in dry
294 conditions (e.g. July) from events that occurred with some rainfall and increased
295 stream discharge (e.g. April) (**Fig. 4b**).

296 MP concentration was calculated as the number of microplastics particles
297 divided by the volume of filtered water ($\text{MP}\cdot\text{m}^{-3}$). We used a linear mixed-effects model
298 (lmm) with sampling event or sampling site as a random factor to test if MP
299 concentration (log-transformed) differs between sampling sites or between sampling
300 event, respectively. A similar model was then used to test the effects of spatial
301 environmental conditions (PC axes: river size and urbanization) on MP concentration,
302 with sampling event as random factor. We then tested the effects of temporal
303 environmental conditions (PC axes: seasonal hydrological conditions and weather
304 changes) on MP concentration, with sampling site as random effect. Fisher Exact test
305 was then used to compare MP colors between MP composition. Spatial and temporal

306 variations in proportion of the three main polymers types (polyethylene, polystyrene,
307 and polypropylene) were tested using generalized mixed-effects models (glmm),
308 considering sampling event and sampling sites as random factors, respectively, using a
309 quasibinomial family. We tested the effects of spatial environmental conditions (PC
310 axes: river size and urbanization) on polymers proportion with sampling event as
311 random factor. Then we tested the effects of temporal environmental conditions (PC
312 axes: seasonal hydrological conditions and weather changes) on polymers proportion,
313 with sampling site as random effect. Linear mixed-effects models with sample code
314 plus sampling event or sampling site as random factor were then used to test for
315 differences in MP size (log-transformed) between sampling sites and sampling events,
316 respectively. Similar models were then used to test the relationship between MP size
317 (log transformed) and spatial and temporal environmental conditions. The relationship
318 between MP size (log-transformed) and the distance to Garonne source was tested
319 using a linear mixed-effect model with sample code and polymer type as random
320 factors. Finally, a linear mixed-effects model (lmm) was used to test differences in MP
321 size (log-transformed) between polymer types, with sample code as random factor.

322 All statistical analyses were performed using R v.4.0.2 (R Core Team, 2019)
323 and linear mixed effects models were performed using the package lme4 v.1.1.10
324 (Bates et al., 2015). Generalized linear mixed-effects models-PQL were performed
325 using the package MASS (Venables et al., 2002). Significant levels of mixed effects
326 models were obtained using the 'Anova' function in the car package (Fox & Weisberg,
327 2019). All explanatory variables were scaled (mean of zero and standard deviation of
328 one) prior to analyses. Assumptions of linearity and homogeneity of variances on
329 residuals from all models were checked visually. All full models were initially run with
330 two-way interactions. As no interaction was significant, models were simplified.

331

332 **3. Results**

3.1 Spatial and temporal variation of MP concentration

A total of 1887 particles were visually detected. Among them, 1283 were within the studied size range (700 μm to 5 mm) and successfully identified by ATR-FTIR as microplastics (**Supplementary Fig. S3**). MP concentration averaged 0.15 $\text{MP}\cdot\text{m}^{-3}$ (\pm 0.46 SD) and ranged from 0 to 3.4 $\text{MP}\cdot\text{m}^{-3}$ across all sampled sites and events. There was overall a significant difference in MP concentration between sampling sites (Imm, $\chi^2 = 170.51$, $p < 0.001$). Specifically, we found that MP concentration was significantly higher in LAU than in TOU site, two sites highly urbanized (**Supplementary Table S1**), that had higher MP concentrations compared to all other sites (post-hoc pairwise comparisons, $p < 0.05$, **Fig. 5a**). There was a significant effect of the level of urbanization on MP concentration (Imm, $\chi^2 = 108.84$, $p < 0.001$), with MP concentration increasing with urbanization (**Supplementary Fig. S6a**). There was no significant effect of river size on MP concentration (Imm, $\chi^2 = 3.43$, $p = 0.064$). There was a significant difference in MP concentration between sampling events (Imm, $\chi^2 = 16.53$, $p < 0.001$) with significantly higher MP concentration in July than in February and October (post-hoc pairwise comparisons, $p < 0.05$, **Fig. 5b**). MP concentration was significantly and positively related to seasonal hydrological conditions with MP concentration increasing in periods of low discharge (Imm, $\chi^2 = 11.20$, $p < 0.001$) (**Supplementary Fig. S6b**). There was no significant effect of weather changes on MP concentration (Imm, $\chi^2 = 2.56$, $p = 0.109$).

3.2 Spatial and temporal variation of MP composition

Three main types of polymers were collected, namely polyethylene (PE), polystyrene (PS) and polypropylene (PP), representing 44.5 %, 30.1 % and 18.2 % of the total number of particles, respectively (**Fig. 6**). The other MP particles represented 7.2 % of all microplastics (**Supplementary Fig.S4**). The three main colors of the MP particles were white, black, and blue, and represented 32.4 %, 31.1 % and 14.3 % of particles,

360 respectively. The other MP particles colors were red (7.6 %), green (6.5 %), yellow (4.5
361 %) and grey (3.6 %).

362 The distribution of particle color significantly differed between polymer types (p
363 < 0.001) with a main contribution of the higher proportion of white particles in the PS
364 (37.9 %) and smaller proportion of white particles in PE (12.7 %) and black particles in
365 PS (10.4 %) (**Fig. 6**).

366 The proportion of PE, the most abundant polymer, among the sampled MP
367 particles was not significantly different between sampling sites (glmm, $\chi^2 = 12.67$, $p =$
368 0.474 , **Supplementary Fig. S7a**). There was a significant difference between sampling
369 events (glmm, $\chi^2 = 11.05$, $p = 0.011$, **Supplementary Fig. S7b**), with a significantly
370 lower proportion of PE measured in October compared to April and July (post-hoc
371 pairwise comparisons, $p < 0.05$). There was no significant relationship between
372 environmental drivers and proportion of PE (**Table 1**). The proportion of PS was not
373 significantly different between sampling sites (glmm, $\chi^2 = 11.60$, $p = 0.561$,
374 **Supplementary Fig. 7c**) and between sampling events (glmm, $\chi^2 = 2.87$, $p = 0.411$,
375 **Supplementary Fig. 7d**). There was no significant effect of environmental variables on
376 the proportion of PS (**Table 1**). There was no significant difference in the proportion of
377 PP between sampling sites (glmm, $\chi^2 = 19.40$ $p = 0.111$, **Supplementary Fig. S7e**)
378 and between sampling events (glmm, $\chi^2 = 6.126$, $p = 0.106$, **Supplementary Fig. S7f**).
379 The proportion of PP was significantly related to river size, with the proportion of PP
380 increasing in larger sites, mainly located more in downstream of the drainage (**Table**
381 **1**). There was no significant effect of the other environmental variables on the
382 proportion of PP (**Table 1**).

383 **3.3 Spatial and temporal variation of MP size**

384 MP size averaged 2.31 mm (± 1.01 SD). There was no significant difference in
385 MP size distribution between sampling sites (lmm, $\chi^2 = 19.34$, $p > 0.05$) (**Fig. 7a**), and

386 no significant effect of urbanization and river size on MP size (Imm, $p > 0.05$). There
387 was a significant difference in MP size between sampling events (Imm, $\chi^2 = 12.91$, $p =$
388 0.005) (**Fig. 7b**), with larger MP in February compared to other sampling events (post-
389 hoc pairwise comparisons, $p < 0.05$). A significant effect of seasonal hydrological
390 conditions in determining the MP size was observed, with MP size decreasing in low
391 hydrological conditions (Imm, $\chi^2 = 8.64$, $p = 0.003$) (**Supplementary Fig. S8**). There
392 was a significant difference in MP size between polymer types (Imm, $\chi^2 = 19.38$, $p <$
393 0.001), with PS being significantly larger than PE and PP (post-hoc test, $p < 0.05$) (**Fig.**
394 **7c**). In the main stream of the Garonne river, MP size significantly decreased when
395 increasing the distance from the Garonne source (Imm, $\chi^2 = 3.909$, $p = 0.048$)
396 (**Supplementary Fig. S9**).

397

398 **4. Discussion**

399 The spatial and temporal dynamics of MP pollution in freshwater ecosystems are
400 complex. We demonstrated that spatial variability in MP concentration observed at the
401 catchment level was driven by urbanization, with MP concentration increasing with
402 urbanization. Temporal variability in MP concentration was strong and driven by
403 seasonal hydrological changes, with higher concentration observed in low flow
404 conditions. We then observed that MP polymers differed in term of color distribution,
405 with higher proportions of white PS and black PE. There was also a temporal variability
406 in the proportion of PE, the most common polymer. The size distribution varied among
407 each polymer, with PS particles being larger. Finally, we found that the temporal
408 variability in MP size was driven by seasonal hydrological changes, with smaller MP
409 encounter in low flow conditions and MP size decreased with the distance to the source
410 only in the main stream of the Garonne River.

411

4.1 Spatial and temporal variability in MP concentration and its determinants

In general, MP pollution in European rivers is highly variable (Li et al., 2020; Wong et al., 2020). The mean MP concentration found in this study (i.e., $0.15 (\pm 0.46) \text{ MP.m}^{-3}$) was within the range of values reported elsewhere, such as in the Rhine catchment ($0.04\text{-}9.97 \text{ MP.m}^{-3}$) (Li et al., 2018; Mani and Burkhardt-Holm, 2019). However, comparisons between studies are limited by differences in size range considered and the use of different methodological approaches, from water sampling to extraction of MP particles. MP pollution is also highly variable within catchments, with difference up to a factor of 250 times (Rodrigues et al., 2018). As predicted, a strong spatial variability in MP pollution was observed within the Garonne catchment and driven by urbanization but not by river size. This result is in agreement with previous findings showing that MP concentration was driven by upstream population size rather than watershed size (Christensen et al., 2020), although in the present study a multivariate approach of environmental conditions was applied. We also found that MP concentration displayed a significant temporal variability, with higher levels of MP pollution observed in low flow conditions. Lower MP abundance in water has previously been associated with weak hydrodynamics conditions in a reservoir and were explained by the reduction in the vertical mixing of MP within the water column (Zhang et al., 2017), with deposition of suspended particles. However, a different mechanism may prevail in our study, probably related with particles size and shape, where low flow conditions results in prevalence of MP in the upper layer of water column and a consequent increase in their measured concentration. Therefore, independently of the global flux of MP, MP pollution level in water surface was reduced in high discharge conditions. Weather changes associated to precipitation prior to field sampling did not affect MP concentration. This is consistent with results observed in the Rhine catchment with no relationship between precipitations and MP concentrations (Mani and Burkhardt-Holm, 2019). A relationship between precipitation and MP concentration

439 was also observed in Tamsui catchment but only in some of the studied rivers (Wong
440 et al., 2020). While precipitation might move MP from land to the rivers, this increase in
441 MP quantity might not translate into significant changes in concentration due to an
442 increased discharge and changes in suspension-settlement dynamics of particles.
443 Studies are therefore still necessary to elucidate the relationship between
444 precipitations, hydrological conditions and MP concentration to understand how the
445 position within the catchment could modulate this relationship.

446

447

448

449

450 **4.2 Spatial and temporal variability in MP type**

451 The diversity of polymer types composing MP are driven by a high diversity of input
452 sources, including plastic industries, littering, roads and wastewater effluent (Grbić et
453 al., 2020; Zhang et al., 2017). In the present study, we found that 92.8% of all MP in
454 the Garonne catchment were composed of three main polymers, PE, PS and PP. This
455 finding is very similar to results observed elsewhere (Mao et al., 2020). These polymers
456 are the most common plastics found in the environment (Wong et al., 2020) and are
457 largely applied in the food packaging, reusable bags, and toys, for example
458 (PlasticsEurope, 2019). Interestingly, this distribution differs from the total European
459 plastic demand, in which these three polymers types represents only 55.4%
460 (PlasticsEurope, 2019), suggesting a difference between the production and this
461 fraction of freshwater MP pollution. The overall lower density of these polymers,
462 commonly lower than the water, might explain their presence in surface water
463 (Andrady, 2017; Wong et al., 2020). However, as these particles are subject to different
464 degradation process while in the environment, that are temporal dynamic and polymer -
465 dependency (Boyle and Örmeci, 2020), their prevalence in water surface might be

466 reduced due to a sedimentation process. For instance, biofouling is known to affect
467 microplastic density, altering their floatability and causing their sedimentation (Karlsson
468 et al., 2018), with studies demonstrating the presence of microplastics composed of
469 low density polymers in river sediments (Van Cauwenberghe et al., 2015). The
470 proportion of PE was higher in low flow conditions, when MP concentration was the
471 highest. Because PE was the main type of polymer observed in the sampled MP,
472 representing almost half of all particles (44.5%), the variation of MP concentration
473 seems to be influenced by the presence of PE particles. We found a significant higher
474 proportion of white PS particles, which is compatible with the higher proportion PS in its
475 foam type (that is, 98% gas and 2% of polystyrene on a volume basis, (Song et al.,
476 2017)) and typically used in packaging or containers (Wang et al., 2019). As most of
477 the PS foam had a spherule shape, their presence in the upper layer of the water
478 column was expected (Van Melkebeke et al., 2020). Moreover, as these particles were
479 weathered only on their surface, a hypothesis of relatively recent emission could be
480 made, as they are expected to easily fragment under mechanical factors (Mani and
481 Burkhardt-Holm, 2019; Song et al., 2017). A comprehensive study of plastic pollution
482 across ecosystem types is essential to identify the potential land sources and transport
483 mechanisms, including the long-term dynamics of MP in the environment, is needed.

484

485 **4.3 Variability in MP size**

486 In streams, MP can be continuously deposited in sediments and resuspended with
487 hydrological dynamics (Rochman and Hoellein, 2020). River banks and floodplains are
488 represent a temporal sink of plastics, where larger MP are more easily trapped
489 (Christensen et al., 2020). Contrary to our predictions, there was no spatial variability of
490 MP size across all sampled sites but MP size was affected by seasonal hydrological
491 conditions with smaller MP in low flow conditions. This finding could be caused by the
492 hydrodynamic processes with larger MP needing higher discharge conditions to be

493 resuspended and transported. At the opposite, the proportion of smaller MP particles,
494 that need less force to be resuspended and/or moved, increased in low discharge
495 conditions. PS particles were, on average, larger than the PP and PE particles which is
496 in line to the hypothesis of a recent emission of PS particles. The size distribution
497 among polymer types was similar to a previous study (Serranti et al., 2018).
498 Temperature and ultraviolet (UV) radiation play an important role in plastic degradation,
499 at a rate largely depending on its exposure (Christensen et al., 2020; Weinstein et al.,
500 2016) and polymer type, that may also be influenced by the manufacturing process
501 (Julienne et al., 2019). Further studies are needed to better understand the specificities
502 of fragmentation mechanisms within rivers.

503 Independently of MP composition and sampling event, a negative correlation
504 between MP size and the distance to the Garonne source was observed. Two mutually
505 non-exclusive hypotheses could explain this finding. First, a possible fragmentation of
506 MP particles could occur along the stream (Garvey et al., 2020; Kataoka et al., 2019).
507 Second, and although it was not measured systematically in the present study, water
508 depth differ between sampling sites. Although water surface was always sampled, this
509 fraction represents a proportion of the water column that varies between each sampling
510 site and event. This may have affected the average size of sampled MP particles in
511 surface water because they are not uniformly distributed throughout the water column
512 (Kooi et al., 2017; Kukulka et al., 2012; Law, 2017). MP particles density, sizes and
513 shapes impact their suspension-settlement dynamics (Daily and Hoffman, 2020).
514 Further studies investigating the vertical (Choy et al., 2019; Liu et al., 2020), through
515 the water column, and lateral (Dris et al., 2015) variability in MP pollution are still
516 needed. The temporal variability in both MP concentration and MP size was driven by
517 hydrological conditions. The increase of MP concentration with decreasing MP size
518 was already reported in water and sediments in coastal metropolis (Su et al., 2020). As
519 particle size decreases, they spread over greater distances, and a wider range of
520 organisms are likely to ingest them (Auta et al., 2017). In addition, because MP

521 abundance increases when their size decreases (Morét-Ferguson et al., 2010; Roch et
522 al., 2019), the size limit (> 700 µm) used in the present study likely underestimates MP
523 pollution. Because MP size is linked to some of their characteristics, it is important to
524 quantify the characteristics (shape, size and polymer composition) of smaller MPs to
525 fully appreciate how MP pollution is linked to their potential effects on freshwater
526 organisms.

527

528 **5. Conclusion**

529 This study identified the main environmental drivers of the variability in MP pollution in
530 a large temperate river and revealed that urbanization and hydrology were the main
531 driver of spatial and temporal variability, respectively. We highlight that not only the
532 concentration or polymer type should be quantified in the analysis of MP pollution
533 because variation in MP properties such as size, density and color, can provide a
534 better understanding of the sources and dynamics of this pollution. The dynamic MP
535 pollution across watersheds, from headwater tributaries to lowland rivers and to its final
536 sink, the marine environment, is complex and multifaceted, and efforts should be made
537 to improve the spatial and temporal resolution of our understanding of MP pollution in
538 aquatic ecosystems for the management of this pollution (Cable et al., 2017; Rochman,
539 2018; Skalska et al., 2020).

540

541 **Author contributions**

542 **Aline Reis de Carvalho** : Collected and analyzed samples, Developed analytical
543 method, Conducted laboratory analyses, Drafted the first version of manuscript;

544 **Flavien Garcia**: Collected and analyzed samples, Conducted laboratory analyses;

545 **Louna Riem-Galliano**: Collected and analyzed samples, Conducted laboratory
546 analyses; **Loïc Tudesque**: Collected and analyzed samples, Collected data; **Magali**

547 **Albignac**: Conducted laboratory analyses; **Alexandra ter Halle**: Designed and

548 supervised the study, Developed analytical method; **Julien Cucherousset**: Designed
549 and supervised the study, Analyzed data, Drafted the first version of manuscript. All
550 authors edited and revised the manuscript.

551

552 **Acknowledgments**

553 We are grateful to our colleagues for their precious help during field work and sample
554 analyses. This study was funded by the Agence de l'Eau Adour-Garonne (PLASTIGAR
555 project) and by the Region Midi-Pyrenees.

556

557

558 **References**

- 559 Andrady, A.L., 2017. The plastic in microplastics: A review. *Marine Pollution Bulletin*
560 119, 12–22. <https://doi.org/10.1016/j.marpolbul.2017.01.082>
- 561 Andrady, A.L., 2011. Microplastics in the marine environment. *Marine Pollution Bulletin*
562 62, 1596–1605. <https://doi.org/10.1016/j.marpolbul.2011.05.030>
- 563 Arthur, C., Baker, J., Bamford, H., 2009. Proceedings of the International Research
564 Workshop on the Occurrence, Effects and Fate of Microplastic Marine Debris.
- 565 Auta, H.S., Emenike, C.U., Fauziah, S.H., 2017. Distribution and importance of
566 microplastics in the marine environment: A review of the sources, fate, effects,
567 and potential solutions. *Environment International* 102, 165–176.
568 <https://doi.org/10.1016/j.envint.2017.02.013>
- 569 Baldwin, A.K., Corsi, S.R., Mason, S.A., 2016. Plastic Debris in 29 Great Lakes
570 Tributaries: Relations to Watershed Attributes and Hydrology. *Environ. Sci.*
571 *Technol.* 50, 10377–10385. <https://doi.org/10.1021/acs.est.6b02917>
- 572 Boyle, K., Örmeci, B., 2020. Microplastics and Nanoplastics in the Freshwater and
573 Terrestrial Environment: A Review. *Water* 12, 2633.
574 <https://doi.org/10.3390/w12092633>
- 575 Cable, R.N., Beletsky, D., Beletsky, R., Wigginton, K., Locke, B.W., Duhaime, M.B.,
576 2017. Distribution and Modeled Transport of Plastic Pollution in the Great
577 Lakes, the World's Largest Freshwater Resource. *Front. Environ. Sci.* 5, 45.
578 <https://doi.org/10.3389/fenvs.2017.00045>
- 579 Chen, H., Jia, Q., Zhao, X., Li, L., Nie, Y., Liu, H., Ye, J., 2020. The occurrence of
580 microplastics in water bodies in urban agglomerations: Impacts of drainage
581 system overflow in wet weather, catchment land-uses, and environmental
582 management practices. *Water Research* 183, 116073.
583 <https://doi.org/10.1016/j.watres.2020.116073>
- 584 Cheung, P.K., Hung, P.L., Fok, L., 2019. River Microplastic Contamination and
585 Dynamics upon a Rainfall Event in Hong Kong, China. *Environ. Process.* 6,
586 253–264. <https://doi.org/10.1007/s40710-018-0345-0>
- 587 Choy, C.A., Robison, B.H., Gagne, T.O., Erwin, B., Firl, E., Halden, R.U., Hamilton,
588 J.A., Katija, K., Lisin, S.E., Rolsky, C., S. Van Houtan, K., 2019. The vertical
589 distribution and biological transport of marine microplastics across the

590 epipelagic and mesopelagic water column. *Sci Rep* 9, 7843.
591 <https://doi.org/10.1038/s41598-019-44117-2>

592 Christensen, N.D., Wisinger, C.E., Maynard, L.A., Chauhan, N., Schubert, J.T., Czuba,
593 J.A., Barone, J.R., 2020. Transport and characterization of microplastics in
594 inland waterways. *Journal of Water Process Engineering* 38, 101640.
595 <https://doi.org/10.1016/j.jwpe.2020.101640>

596 Cole, M., Lindeque, P., Halsband, C., Galloway, T.S., 2011. Microplastics as
597 contaminants in the marine environment: A review. *Marine Pollution Bulletin* 62,
598 2588–2597. <https://doi.org/10.1016/j.marpolbul.2011.09.025>

599 Collard, F., Gasperi, J., Gabrielsen, G.W., Tassin, B., 2019. Plastic Particle Ingestion
600 by Wild Freshwater Fish: A Critical Review. *Environ. Sci. Technol.* 53, 12974–
601 12988. <https://doi.org/10.1021/acs.est.9b03083>

602 Couceiro, S.R.M., Hamada, N., Luz, S.L.B., Forsberg, B.R., Pimentel, T.P., 2007.
603 Deforestation and sewage effects on aquatic macroinvertebrates in urban
604 streams in Manaus, Amazonas, Brazil. *Hydrobiologia* 575, 271–284.
605 <https://doi.org/10.1007/s10750-006-0373-z>

606 Daily, J., Hoffman, M.J., 2020. Modeling the three-dimensional transport and
607 distribution of multiple microplastic polymer types in Lake Erie. *Marine Pollution*
608 *Bulletin* 154, 111024. <https://doi.org/10.1016/j.marpolbul.2020.111024>

609 Dehaut, A., Cassone, A.-L., Frère, L., Hermabessiere, L., Himber, C., Rinnert, E.,
610 Rivière, G., Lambert, C., Soudant, P., Huvet, A., Duflos, G., Paul-Pont, I., 2016.
611 Microplastics in seafood: Benchmark protocol for their extraction and
612 characterization. *Environmental Pollution* 215, 223–233.
613 <https://doi.org/10.1016/j.envpol.2016.05.018>

614 Dris, R., Gasperi, J., Rocher, V., Saad, M., Renault, N., Tassin, B., 2015. Microplastic
615 contamination in an urban area: a case study in Greater Paris. *Environ. Chem.*
616 12, 592–599. <https://doi.org/10.1071/EN14167>

617 Eerkes-Medrano, D., Thompson, R., 2018. Occurrence, Fate, and Effect of
618 Microplastics in Freshwater Systems, in: *Microplastic Contamination in Aquatic*
619 *Environments*. Elsevier, pp. 95–132. <https://doi.org/10.1016/B978-0-12-813747-5.00004-7>

620 Eerkes-Medrano, D., Thompson, R.C., Aldridge, D.C., 2015. Microplastics in
621 freshwater systems: A review of the emerging threats, identification of
622 knowledge gaps and prioritisation of research needs. *Water Research* 75, 63–
623 82. <https://doi.org/10.1016/j.watres.2015.02.012>

624 Eo, S., Hong, S.H., Song, Y.K., Han, G.M., Shim, W.J., 2019. Spatiotemporal
625 distribution and annual load of microplastics in the Nakdong River, South
626 Korea. *Water Research* 160, 228–237.
627 <https://doi.org/10.1016/j.watres.2019.05.053>

628 European Environment Agency, 2018. CORINE Land Cover. Commission of the
629 European Communities.

630 Faure, F., Corbaz, M., Baecher, H., Felipe, L., 2012. Pollution due to plastics and
631 microplastics in Lake Geneva and in the Mediterranean Sea. *ARCHIVES DES*
632 *SCIENCES* 7.

633 Foley, C.J., Feiner, Z.S., Malinich, T.D., Höök, T.O., 2018. A meta-analysis of the
634 effects of exposure to microplastics on fish and aquatic invertebrates. *Science*
635 *of The Total Environment* 631–632, 550–559.
636 <https://doi.org/10.1016/j.scitotenv.2018.03.046>

637 Galgani, F., Hanke, G., Werner, S., De Vrees, L., 2013. Marine litter within the
638 European Marine Strategy Framework Directive. *ICES Journal of Marine*
639 *Science* 70, 1055–1064. <https://doi.org/10.1093/icesjms/fst122>

640 Gallardo, B., Clavero, M., Sánchez, M.I., Vilà, M., 2016. Global ecological impacts of
641 invasive species in aquatic ecosystems. *Glob Change Biol* 22, 151–163.
642 <https://doi.org/10.1111/gcb.13004>

643

644 Garvey, C.J., Impéror-Clerc, M., Rouzière, S., Gouadec, G., Boyron, O., Roweczyk,
645 L., Mingotaud, A.F., ter Halle, A., 2020. Molecular-Scale Understanding of the
646 Embrittlement in Polyethylene Ocean Debris. *Environ. Sci. Technol.* 54, 11173–
647 11181. <https://doi.org/10.1021/acs.est.0c02095>
648 Géoportail [WWW Document], 2020. URL <https://www.geoportail.gouv.fr/> (accessed
649 9.29.20).

650 Gewert, B., Plasmann, M.M., MacLeod, M., 2015. Pathways for degradation of plastic
651 polymers floating in the marine environment. *Environ. Sci.: Processes Impacts*
652 17, 1513–1521. <https://doi.org/10.1039/C5EM00207A>

653 Grbić, J., Helm, P., Athey, S., Rochman, C., 2020. Microplastics entering northwestern
654 Lake Ontario are diverse and linked to urban sources. *Water Research* 115623.
655 <https://doi.org/10.1016/j.watres.2020.115623>

656 Han, M., Niu, X., Tang, M., Zhang, B.-T., Wang, G., Yue, W., Kong, X., Zhu, J., 2020.
657 Distribution of microplastics in surface water of the lower Yellow River near
658 estuary. *Science of The Total Environment* 707, 135601.
659 <https://doi.org/10.1016/j.scitotenv.2019.135601>

660 Hartmann, N.B., Hüffer, T., Thompson, R.C., Hassellöv, M., Verschoor, A., Daugaard,
661 A.E., Rist, S., Karlsson, T., Brennholt, N., Cole, M., Herrling, M.P., Hess, M.C.,
662 Ivleva, N.P., Lusher, A.L., Wagner, M., 2019. Are We Speaking the Same
663 Language? Recommendations for a Definition and Categorization Framework
664 for Plastic Debris. *Environ. Sci. Technol.* 53, 1039–1047.
665 <https://doi.org/10.1021/acs.est.8b05297>

666 Hidalgo-Ruz, V., Gutow, L., Thompson, R.C., Thiel, M., 2012. Microplastics in the
667 Marine Environment: A Review of the Methods Used for Identification and
668 Quantification. *Environ. Sci. Technol.* 46, 3060–3075.
669 <https://doi.org/10.1021/es2031505>

670 Hofland, A., 2012. Alkyd resins: From down and out to alive and kicking. *Progress in*
671 *Organic Coatings* 73, 274–282. <https://doi.org/10.1016/j.porgcoat.2011.01.014>

672 Horton, A.A., Walton, A., Spurgeon, D.J., Lahive, E., Svendsen, C., 2017. Microplastics
673 in freshwater and terrestrial environments: Evaluating the current understanding
674 to identify the knowledge gaps and future research priorities. *Science of The*
675 *Total Environment* 586, 127–141.
676 <https://doi.org/10.1016/j.scitotenv.2017.01.190>

677 Huppertsberg, S., Knepper, T.P., 2020. Validation of an FT-IR Microscopy Method for
678 the Determination of Microplastic Particles in Surface Waters. *MethodsX*
679 100874. <https://doi.org/10.1016/j.mex.2020.100874>

680 Hurley, R., Woodward, J., Rothwell, J.J., 2018. Microplastic contamination of river beds
681 significantly reduced by catchment-wide flooding. *Nature Geoscience* 11, 251–
682 257. <https://doi.org/10.1038/s41561-018-0080-1>

683 HydroEauFrance [WWW Document], 2020. . Hydro Eau France. URL
684 <http://www.hydro.eaufrance.fr/> (accessed 9.29.20).

685 INSEE, 2018. Institut National de la Statistique et des Etudes Economiques.

686 Järllskog, I., 2020. Occurrence of tire and bitumen wear microplastics on urban streets
687 and in sweepsand and washwater. *Science of the Total Environment* 13.

688 Julienne, F., Delorme, N., Lagarde, F., 2019. From macroplastics to microplastics: Role
689 of water in the fragmentation of polyethylene. *Chemosphere* 236, 124409.
690 <https://doi.org/10.1016/j.chemosphere.2019.124409>

691 Käßler, A., Fischer, D., Oberbeckmann, S., Schernewski, G., Labrenz, M., Eichhorn,
692 K.-J., Voit, B., 2016. Analysis of environmental microplastics by vibrational
693 microspectroscopy: FTIR, Raman or both? *Anal Bioanal Chem* 408, 8377–
694 8391. <https://doi.org/10.1007/s00216-016-9956-3>

695 Karlsson, T.M., Hassellöv, M., Jakubowicz, I., 2018. Influence of thermooxidative
696 degradation on the in situ fate of polyethylene in temperate coastal waters.
697 *Marine Pollution Bulletin* 135, 187–194.
698 <https://doi.org/10.1016/j.marpolbul.2018.07.015>

699 Karlsson, T.M., Vethaak, A.D., Almroth, B.C., Ariese, F., van Velzen, M., Hassellöv, M.,
700 Leslie, H.A., 2017. Screening for microplastics in sediment, water, marine
701 invertebrates and fish: Method development and microplastic accumulation.
702 *Marine Pollution Bulletin* 122, 403–408.
703 <https://doi.org/10.1016/j.marpolbul.2017.06.081>

704 Kataoka, T., Nihei, Y., Kudou, K., Hinata, H., 2019. Assessment of the sources and
705 inflow processes of microplastics in the river environments of Japan.
706 *Environmental Pollution* 244, 958–965.
707 <https://doi.org/10.1016/j.envpol.2018.10.111>

708 Kooi, M., Nes, E.H. van, Scheffer, M., Koelmans, A.A., 2017. Ups and Downs in the
709 Ocean: Effects of Biofouling on Vertical Transport of Microplastics. *Environ. Sci.*
710 *Technol.* 51, 7963–7971. <https://doi.org/10.1021/acs.est.6b04702>

711 Kukulka, T., Proskurowski, G., Morét-Ferguson, S., Meyer, D.W., Law, K.L., 2012. The
712 effect of wind mixing on the vertical distribution of buoyant plastic debris: WIND
713 EFFECTS ON PLASTIC MARINE DEBRIS. *Geophys. Res. Lett.* 39, n/a-n/a.
714 <https://doi.org/10.1029/2012GL051116>

715 Lambs, L., Brunet, F., Probst, J.-L., 2009. Isotopic characteristics of the Garonne River
716 and its tributaries. *Rapid Commun. Mass Spectrom.* 23, 2543–2550.
717 <https://doi.org/10.1002/rcm.4102>

718 Law, K.L., 2017. Plastics in the Marine Environment. *Annu. Rev. Mar. Sci.* 9, 205–229.
719 <https://doi.org/10.1146/annurev-marine-010816-060409>

720 Leads, R.R., Weinstein, J.E., 2019. Occurrence of tire wear particles and other
721 microplastics within the tributaries of the Charleston Harbor Estuary, South
722 Carolina, USA. *Marine Pollution Bulletin* 145, 569–582.
723 <https://doi.org/10.1016/j.marpolbul.2019.06.061>

724 Lebreton, L.C.M., van der Zwet, J., Damsteeg, J.-W., Slat, B., Andrady, A., Reisser, J.,
725 2017. River plastic emissions to the world's oceans. *Nat Commun* 8, 15611.
726 <https://doi.org/10.1038/ncomms15611>

727 Li, C., Busquets, R., Campos, L.C., 2020. Assessment of microplastics in freshwater
728 systems: A review. *Science of The Total Environment* 707, 135578.
729 <https://doi.org/10.1016/j.scitotenv.2019.135578>

730 Li, J., Liu, H., Paul Chen, J., 2018. Microplastics in freshwater systems: A review on
731 occurrence, environmental effects, and methods for microplastics detection.
732 *Water Research* 137, 362–374. <https://doi.org/10.1016/j.watres.2017.12.056>

733 Liu, K., Courteney-Jones, W., Wang, X., Song, Z., Wei, N., Li, D., 2020. Elucidating the
734 vertical transport of microplastics in the water column: A review of sampling
735 methodologies and distributions. *Water Research* 186, 116403.
736 <https://doi.org/10.1016/j.watres.2020.116403>

737 Lusher, A.L., Tirelli, V., O'Connor, I., Officer, R., 2015. Microplastics in Arctic polar
738 waters: the first reported values of particles in surface and sub-surface
739 samples. *Sci Rep* 5, 14947. <https://doi.org/10.1038/srep14947>

740 Magnuson, J.J., Webster, K.E., Assel, R.A., Bowser, C.J., Dillon, P.J., Eaton, J.G.,
741 Evans, H.E., Fee, E.J., Hall, R.I., Mortsch, L.R., Schindler, D.W., Quinn, F.H.,
742 1997. Potencial effects of climate changes on aquatic systems: Laurentian
743 Great Lakes and Precambrian shield region. *Hydrological Processes* 11, 47.

744 Maire, A., Buisson, L., Biau, S., Canal, J., Laffaille, P., 2013. A multi-faceted framework
745 of diversity for prioritizing the conservation of fish assemblages. *Ecological*
746 *Indicators* 34, 450–459. <https://doi.org/10.1016/j.ecolind.2013.06.009>

747 Mani, T., Burkhardt-Holm, P., 2019. Seasonal microplastics variation in nival and
748 pluvial stretches of the Rhine River – From the Swiss catchment towards the
749 North Sea. *Science of The Total Environment* 135579.
750 <https://doi.org/10.1016/j.scitotenv.2019.135579>

751 Mao, Y., Li, H., Gu, W., Yang, G., Liu, Y., He, Q., 2020. Distribution and characteristics
752 of microplastics in the Yulin River, China: Role of environmental and spatial

753 factors. *Environmental Pollution* 265, 115033.
754 <https://doi.org/10.1016/j.envpol.2020.115033>

755 McNeish, R.E., Kim, L.H., Barrett, H.A., Mason, S.A., Kelly, J.J., Hoellein, T.J., 2018.
756 Microplastic in riverine fish is connected to species traits. *Sci Rep* 8, 11639.
757 <https://doi.org/10.1038/s41598-018-29980-9>

758 MeteoFrance [WWW Document], 2020. . METEO-FRANCE : Publiothèque. URL
759 <https://publitheque.meteo.fr/okapi/accueil/okapiWebPubli/index.jsp> (accessed
760 9.29.20).

761 Morét-Ferguson, S., Law, K.L., Proskurowski, G., Murphy, E.K., Peacock, E.E., Reddy,
762 C.M., 2010. The size, mass, and composition of plastic debris in the western
763 North Atlantic Ocean. *Marine Pollution Bulletin* 60, 1873–1878.
764 <https://doi.org/10.1016/j.marpolbul.2010.07.020>

765 Morita, K., Morita, S.H., Yamamoto, S., 2009. Effects of habitat fragmentation by
766 damming on salmonid fishes: lessons from white-spotted charr in Japan. *Ecol*
767 *Res* 24, 711–722. <https://doi.org/10.1007/s11284-008-0579-9>

768 PlasticsEurope, 2019. PlasticsEurope - The Facts 2019 [WWW Document]. URL
769 [https://www.plasticseurope.org/fr/resources/publications/1804-plastics-facts-](https://www.plasticseurope.org/fr/resources/publications/1804-plastics-facts-2019)
770 [2019](https://www.plasticseurope.org/fr/resources/publications/1804-plastics-facts-2019) (accessed 9.14.20).

771 Polymer Database [WWW Document], 2020. . Polymer Database. URL
772 <http://polymerdatabase.com/home.html> (accessed 9.29.20).

773 Prata, J.C., da Costa, J.P., Lopes, I., Duarte, A.C., Rocha-Santos, T., 2020.
774 Environmental exposure to microplastics: An overview on possible human
775 health effects. *Science of The Total Environment* 702, 134455.
776 <https://doi.org/10.1016/j.scitotenv.2019.134455>

777 R Core Team, 2019. R: A Language and Environment for Statistical Computing. R
778 Foundation for Statistical Computing, Vienna, Austria.

779 Rasband, W.S., 1997. ImageJ. U. S. National Institutes of Health, Bethesda, Maryland,
780 USA. <https://imagej.nih.gov/ij/>.

781 Roch, S., Walter, T., Ittner, L.D., Friedrich, C., Brinker, A., 2019. A systematic study of
782 the microplastic burden in freshwater fishes of south-western Germany - Are we
783 searching at the right scale? *Science of The Total Environment* 689, 1001–
784 1011. <https://doi.org/10.1016/j.scitotenv.2019.06.404>

785 Rochman, C.M., 2018. Microplastics research—from sink to source. *Science* 360, 28–
786 29. <https://doi.org/10.1126/science.aar7734>

787 Rochman, C.M., Hoellein, T., 2020. The global odyssey of plastic pollution. *Science*
788 368, 1184–1185. <https://doi.org/10.1126/science.abc4428>

789 Rodrigues, M.O., Abrantes, N., Gonçalves, F.J.M., Nogueira, H., Marques, J.C.,
790 Gonçalves, A.M.M., 2018. Spatial and temporal distribution of microplastics in
791 water and sediments of a freshwater system (Antuã River, Portugal). *Science of*
792 *The Total Environment* 633, 1549–1559.
793 <https://doi.org/10.1016/j.scitotenv.2018.03.233>

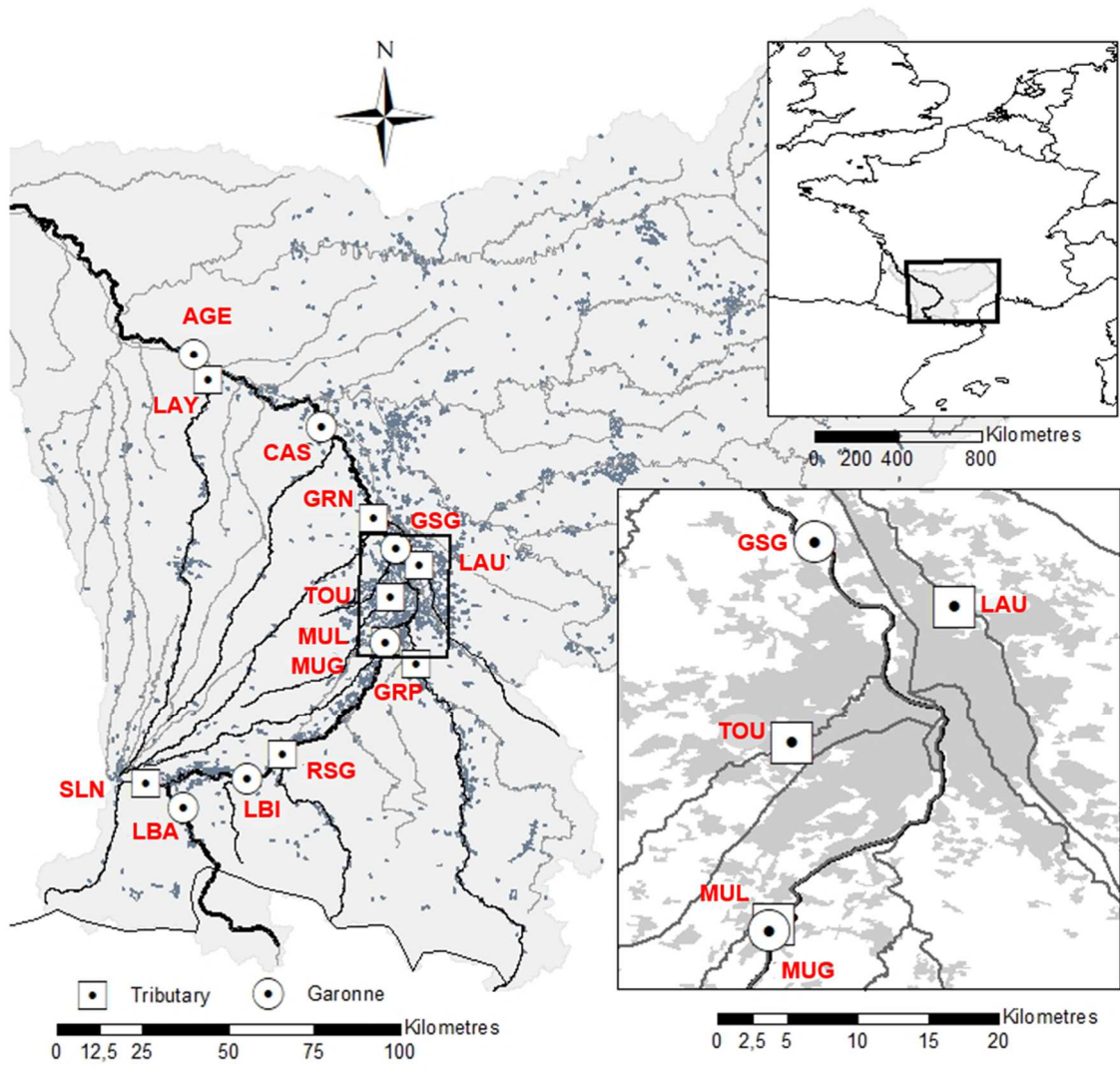
794 Serranti, S., Palmieri, R., Bonifazi, G., Cózar, A., 2018. Characterization of microplastic
795 litter from oceans by an innovative approach based on hyperspectral imaging.
796 *Waste Management* 76, 117–125.
797 <https://doi.org/10.1016/j.wasman.2018.03.003>

798 Skalska, K., Ockelford, A., Ebdon, J.E., Cundy, A.B., 2020. Riverine microplastics:
799 Behaviour, spatio-temporal variability, and recommendations for standardised
800 sampling and monitoring. *Journal of Water Process Engineering* 38, 101600.
801 <https://doi.org/10.1016/j.jwpe.2020.101600>

802 Sloommaekers, B., Catarci Carteny, C., Belpaire, C., Saverwyns, S., Fremout, W., Blust,
803 R., Bervoets, L., 2019. Microplastic contamination in gudgeons (*Gobio gobio*)
804 from Flemish rivers (Belgium). *Environmental Pollution* 244, 675–684.
805 <https://doi.org/10.1016/j.envpol.2018.09.136>

- 806 Smith, M., Love, D.C., Rochman, C.M., Neff, R.A., 2018. Microplastics in Seafood and
807 the Implications for Human Health. *Curr Envir Health Rpt* 5, 375–386.
808 <https://doi.org/10.1007/s40572-018-0206-z>
- 809 Song, Y.K., Hong, S.H., Jang, M., Han, G.M., Jung, S.W., Shim, W.J., 2017. Combined
810 Effects of UV Exposure Duration and Mechanical Abrasion on Microplastic
811 Fragmentation by Polymer Type. *Environ. Sci. Technol.* 51, 4368–4376.
812 <https://doi.org/10.1021/acs.est.6b06155>
- 813 Song, Y.K., Hong, S.H., Jang, M., Kang, J.-H., Kwon, O.Y., Han, G.M., Shim, W.J.,
814 2014. Large Accumulation of Micro-sized Synthetic Polymer Particles in the Sea
815 Surface Microlayer. *Environ. Sci. Technol.* 48, 9014–9021.
816 <https://doi.org/10.1021/es501757s>
- 817 Su, L., Sharp, S.M., Pettigrove, V.J., Craig, N.J., Nan, B., Du, F., Shi, H., 2020.
818 Superimposed microplastic pollution in a coastal metropolis. *Water Research*
819 168, 115140. <https://doi.org/10.1016/j.watres.2019.115140>
- 820 ter Halle, A., Ladirat, L., Martignac, M., Mingotaud, A.F., Boyron, O., Perez, E., 2017.
821 To what extent are microplastics from the open ocean weathered?
822 *Environmental Pollution* 227, 167–174.
823 <https://doi.org/10.1016/j.envpol.2017.04.051>
- 824 Thompson, R.C., Moore, C.J., vom Saal, F.S., Swan, S.H., 2009. Plastics, the
825 environment and human health: current consensus and future trends. *Phil.*
826 *Trans. R. Soc. B* 364, 2153–2166. <https://doi.org/10.1098/rstb.2009.0053>
- 827 Van Cauwenberghe, L., Devriese, L., Galgani, F., Robbins, J., Janssen, C.R., 2015.
828 Microplastics in sediments: A review of techniques, occurrence and effects.
829 *Marine Environmental Research* 111, 5–17.
830 <https://doi.org/10.1016/j.marenvres.2015.06.007>
- 831 Van Melkebeke, M., Janssen, C.R., De Meester, S., 2020. Characteristics and Sinking
832 Behavior of Typical Microplastics including the Potential Effect of Biofouling:
833 Implications for Remediation. *Environ. Sci. Technol.* *acs.est.9b07378*.
834 <https://doi.org/10.1021/acs.est.9b07378>
- 835 Venables, W.N., Ripley, B.D., Venables, W.N., 2002. *Modern applied statistics with S*,
836 4th ed. ed, *Statistics and computing*. Springer, New York.
- 837 Verschoor, A., de Poorter, L., Dröge, R., Kuenen, J., de Valk, E., 2016. Emission of
838 microplastics and potential mitigation measures. *National Institute for Public*
839 *Health and the Environmental* 76.
- 840 Vörösmarty, C.J., McIntyre, P.B., Gessner, M.O., Dudgeon, D., Prusevich, A., Green,
841 P., Glidden, S., Bunn, S.E., Sullivan, C.A., Liermann, C.R., Davies, P.M., 2010.
842 Global threats to human water security and river biodiversity. *Nature* 467, 555–
843 561. <https://doi.org/10.1038/nature09440>
- 844 Wang, T., Zou, X., Li, B., Yao, Y., Zang, Z., Li, Y., Yu, W., Wang, W., 2019. Preliminary
845 study of the source apportionment and diversity of microplastics: Taking floating
846 microplastics in the South China Sea as an example. *Environmental Pollution*
847 245, 965–974. <https://doi.org/10.1016/j.envpol.2018.10.110>
- 848 Weinstein, J.E., Crocker, B.K., Gray, A.D., 2016. From macroplastic to microplastic:
849 Degradation of high-density polyethylene, polypropylene, and polystyrene in a
850 salt marsh habitat: Degradation of plastic in a salt marsh habitat. *Environ*
851 *Toxicol Chem* 35, 1632–1640. <https://doi.org/10.1002/etc.3432>
- 852 Windsor, F.M., Tilley, R.M., Tyler, C.R., Ormerod, S.J., 2019. Microplastic ingestion by
853 riverine macroinvertebrates. *Science of The Total Environment* 646, 68–74.
854 <https://doi.org/10.1016/j.scitotenv.2018.07.271>
- 855 Wong, G., Löwemark, L., Kunz, A., 2020. Microplastic pollution of the Tamsui River and
856 its tributaries in northern Taiwan: Spatial heterogeneity and correlation with
857 precipitation. *Environmental Pollution* 260, 113935.
858 <https://doi.org/10.1016/j.envpol.2020.113935>
- 859 Wong, J.K.H., Lee, K.K., Tang, K.H.D., Yap, P.-S., 2020. Microplastics in the
860 freshwater and terrestrial environments: Prevalence, fates, impacts and

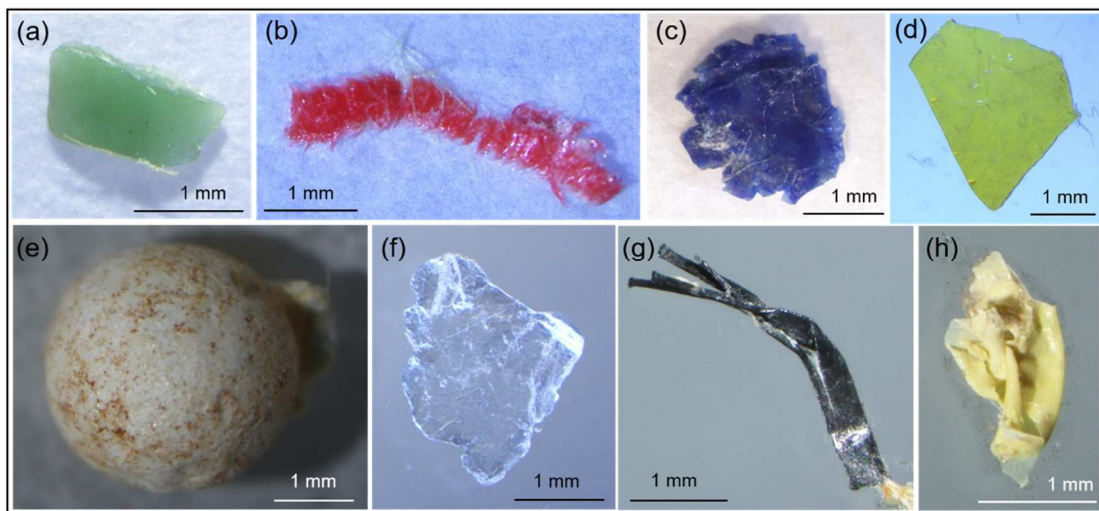
861 sustainable solutions. *Science of The Total Environment* 719, 137512.
862 <https://doi.org/10.1016/j.scitotenv.2020.137512>
863 Woodall, L.C., Sanchez-Vidal, A., Canals, M., Paterson, G.L.J., Coppock, R., Sleight,
864 V., Calafat, A., Rogers, A.D., Narayanaswamy, B.E., Thompson, R.C., 2014.
865 The deep sea is a major sink for microplastic debris. *R. Soc. open sci.* 1,
866 140317. <https://doi.org/10.1098/rsos.140317>
867 Wu, P., Tang, Y., Dang, M., Wang, S., Jin, H., Liu, Y., Jing, H., Zheng, C., Yi, S., Cai,
868 Z., 2019. Spatial-Temporal Distribution of Microplastics in Surface Water and
869 Sediments of Maozhou River within Guangdong-Hong Kong-Macao Greater
870 Bay Area. *Science of The Total Environment* 135187.
871 <https://doi.org/10.1016/j.scitotenv.2019.135187>
872 Yonkos, L.T., Friedel, E.A., Perez-Reyes, A.C., Ghosal, S., Arthur, C.D., 2014.
873 Microplastics in Four Estuarine Rivers in the Chesapeake Bay, U.S.A. *Environ.*
874 *Sci. Technol.* 48, 14195–14202. <https://doi.org/10.1021/es5036317>
875 Zhang, K., Xiong, X., Hu, H., Wu, C., Bi, Y., Wu, Y., Zhou, B., Lam, P.K.S., Liu, J.,
876 2017. Occurrence and Characteristics of Microplastic Pollution in Xiangxi Bay of
877 Three Gorges Reservoir, China. *Environ. Sci. Technol.* 51, 3794–3801.
878 <https://doi.org/10.1021/acs.est.7b00369>
879
880



1
2
3

Figure 1. Map of the study area and localization of the sampling sites.

4



5

6 **Figure 2.** Examples of microplastics collected in surface water samples in the Garonne

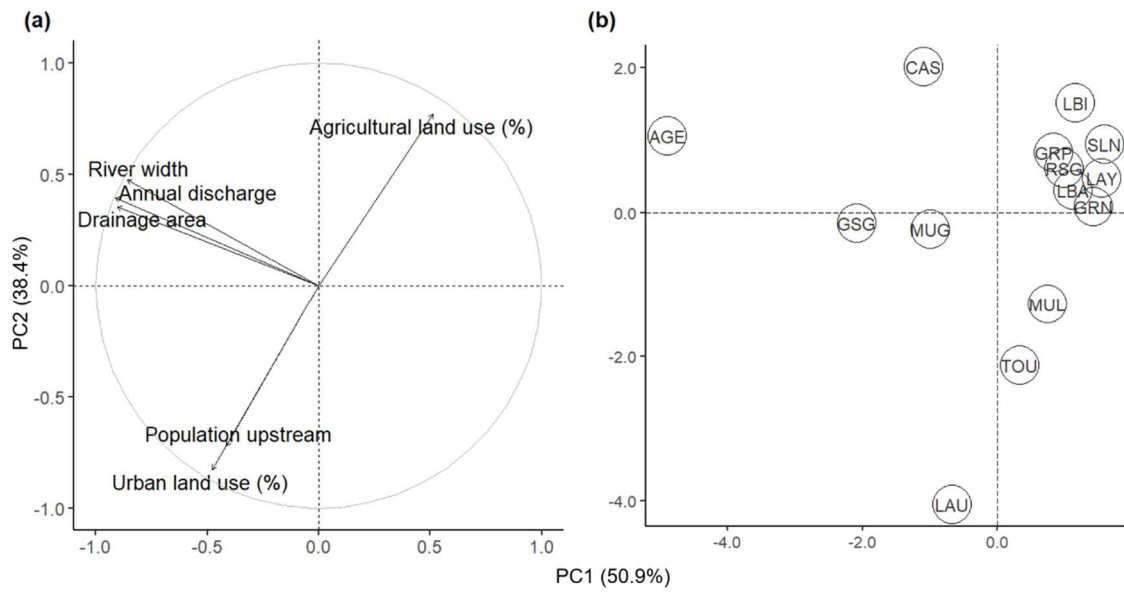
7 River: (A) green polystyrene; (B) red polyester; (C) blue polyethylene; (D) yellow

8 polyethylene; (E) white polystyrene; (F) white polypropylene; (G) black polypropylene

9 and (H) yellow polyurethane

10

11

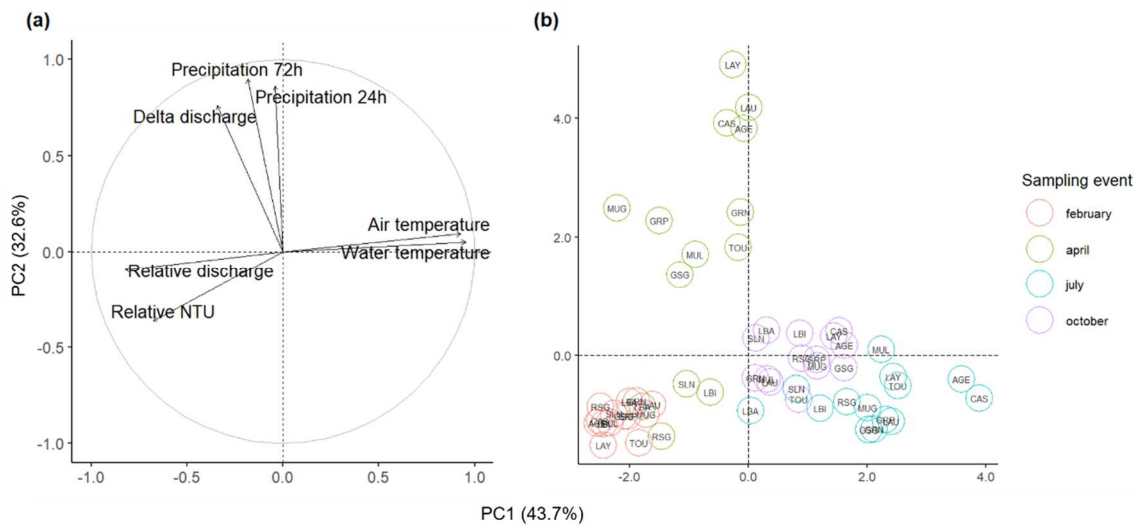


12

13 **Figure 3.** Environmental conditions across the studied sites: (a) correlation circle for
14 spatial variables and (b) distribution of sampling sites along PC1 (river size) and PC2
15 (urbanization) axes.

16

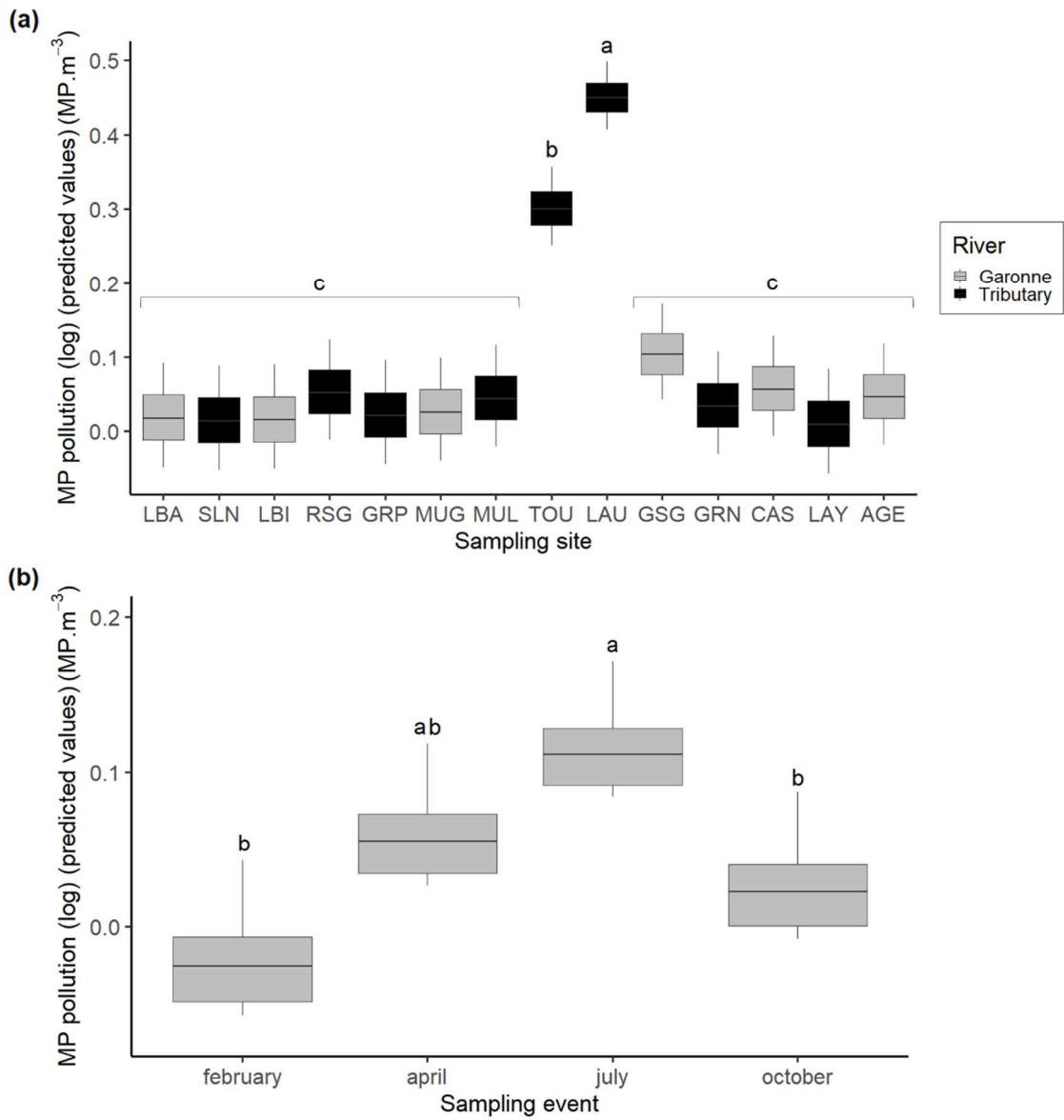
17



18

19 **Figure 4.** Environmental conditions across sampling events: (a) correlation circle for
20 temporal variables and (b) distribution of sampling events along PC1 (seasonal
21 hydrological conditions) and PC2 (weather changes) axes.

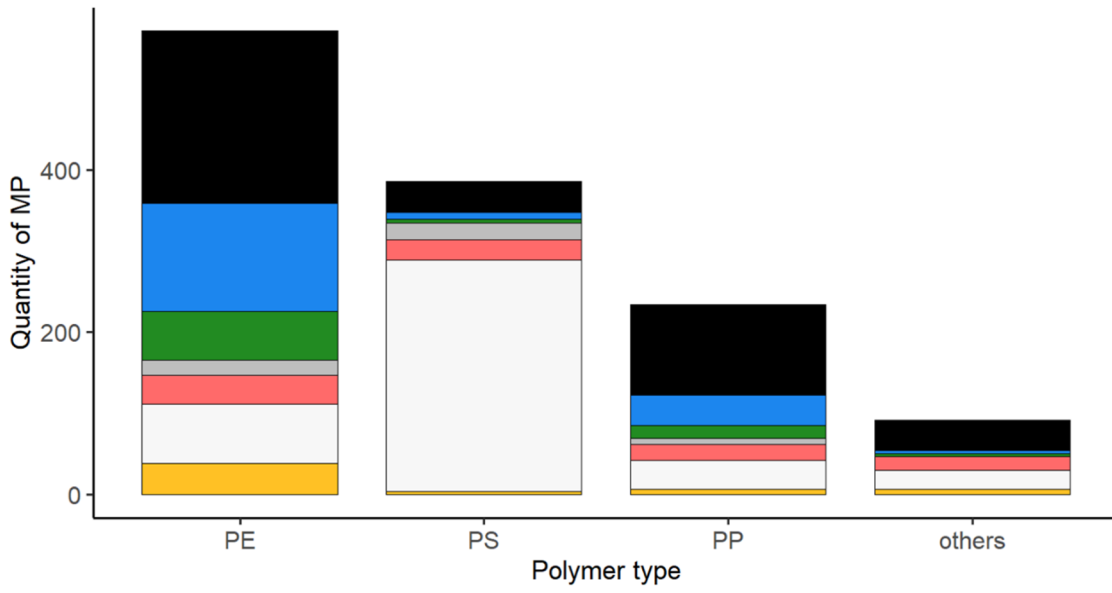
22



24

25 **Figure 5.** Variability of microplastic concentration (log-transformed, MP.m⁻³) between
 26 (a) sampling sites (from upstream to downstream), and (b) sampling events. Different
 27 letters indicate significant differences (p < 0.05).

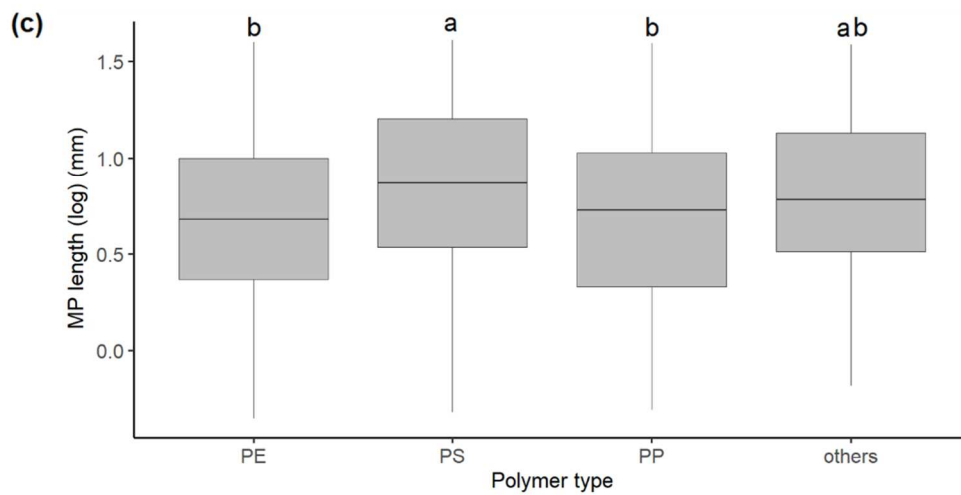
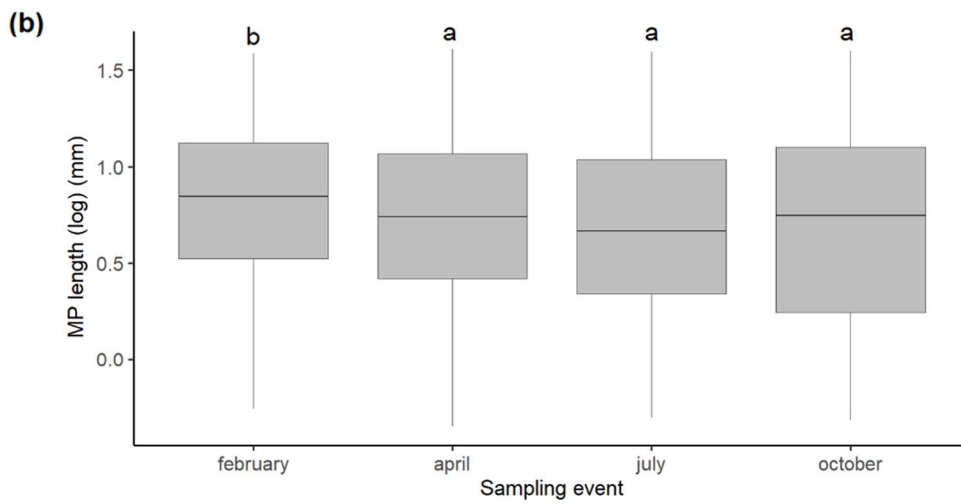
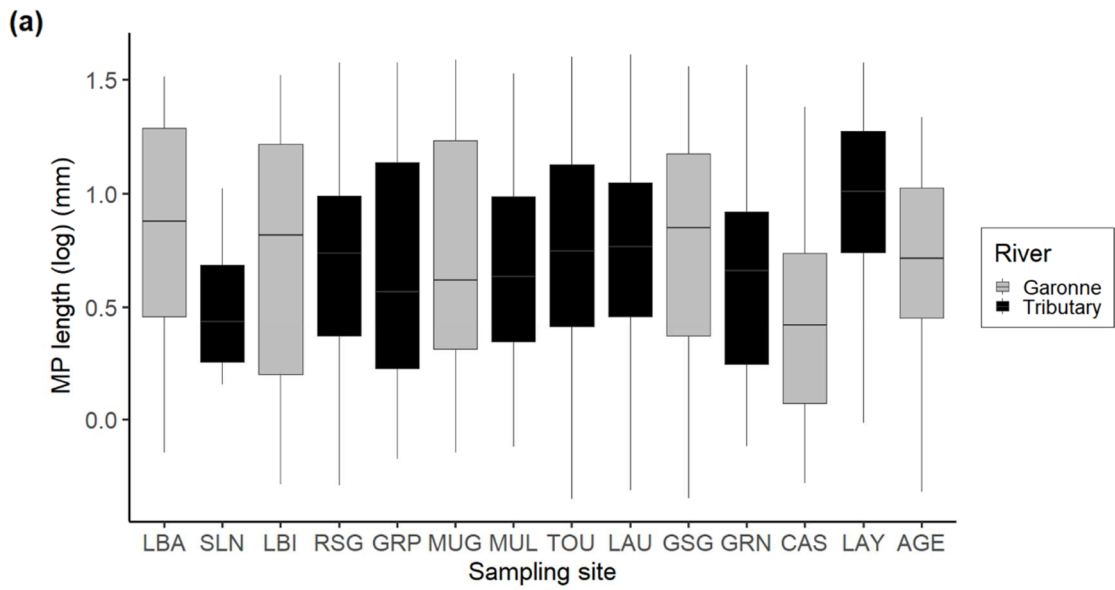
28



29

30 **Figure 6.** Distribution of particles colors for each polymer type. Displayed colors
 31 represent particles colors (black, blue, green, grey, red, white and yellow, respectively).

32



33

34

35

36

Figure 7. Microplastic size (log-transformed, mm) between (a) sampling sites, (b) sampling events and (c) polymer type. Different letters indicate significant differences ($p < 0.05$).

- 1 **Table 1.** Results of the mixed effect models testing the effects of environmental
 2 conditions of the proportion of the three main polymer types (PE, PS and PP).

Response	Spatial variability			Temporal variability		
	<i>Parameter</i>	<i>t</i>	<i>P</i>	<i>Parameter</i>	<i>t</i>	<i>p</i>
PE proportion	<i>Urbanization</i>	1.176	0.241	<i>Seasonal changes</i>	-0.014	0.988
	<i>River size</i>	-0.589	0.557	<i>Weather changes</i>	-0.664	0.507
	<i>Intercept</i>	-2.484	0.014	<i>Intercept</i>	-2.266	0.024
PS proportion	<i>Urbanization</i>	1.468	0.144	<i>Seasonal changes</i>	-0.119	0.905
	<i>River size</i>	1.929	0.055	<i>Weather changes</i>	-0.383	0.702
	<i>Intercept</i>	-10.254	0.000	<i>Intercept</i>	-10.605	0.000
PP proportion	<i>Urbanization</i>	1.001	0.318	<i>Seasonal changes</i>	-0.466	0.642
	<i>River size</i>	2.485	0.014	<i>Weather changes</i>	0.898	0.370
	<i>Intercept</i>	-10.225	0.000	<i>Intercept</i>	-11.441	0.000

3

